



Contents lists available at ScienceDirect

Chemical Physics Letters

journal homepage: www.elsevier.com/locate/cplett

Design and photophysical properties of a new molecule with a N–B–N linked chromophore

Snezhana Bakalova^a, Francisco Mendicuti^b, Obis Castaño^b, Jose Kaneti^{a,b,*}

^a Institute of Organic Chemistry with Centre of Phytochemistry, Bulgarian Academy of Sciences, Acad. G. Bonchev Str., Block 9, 1113 Sofia, Bulgaria

^b Department of Physical Chemistry, University of Alcalá, 28871 Alcalá de Henares, Madrid, Spain

ARTICLE INFO

Article history:

Received 29 May 2009

In final form 26 July 2009

Available online xxxxx

ABSTRACT

A new heterocyclic system, pyrido[6,5-a]boratriazine, has been designed with the aid of TD DFT (TDA) and other quantum mechanical calculations aiming at tunable UV–Vis–Near IR absorption and intense fluorescence, conveniently sensitive to the environment. Special emphasis has been put on solvent effects on the mentioned electronic transition energies and intensities.

© 2009 Elsevier B.V. All rights reserved.

1. Introduction

A class of heterocycles possessing the N–B–N linkage, borindacenes **1**, has recently come to prominence as the result of their excellent photochemical stability and intense fluorescence. Since the initial commercialization of borindacene derivatives under the trade name BODIPY[®], these N–B–N containing molecules have become increasingly popular and have been used in any imaginable fluorescence-based application, starting with analytical uses as ion, molecule and protein sensors, and going further to biomedical indicators and fluorescence imaging, photoelectronic materials and nanodevice components [1–4]. Along with their remarkably high absorption coefficients, fluorescence quantum yields and photostability, Förster photoexcitation energy transfer capabilities, FRET, and negligible triplet-state excitations, BODIPY dyes also possess several important shortcomings – small Stokes' shifts, low solubility in water, self-quenching [4] and low sensitivity to medium effects [2–4]. While new borindacene derivatives are currently intensively synthesized and studied, there is still an open field to the design of new B–N chromophores with possibly improved photochemical stability, photophysical properties and solubility, as well as FRET capabilities comparable or even better than, for example, the existing BODIPY dual chromophore dyes [5,6] (see Scheme 1).

Apart of the mentioned borindacene **1** N–B–N derivatives, commercialized under the trademark BODIPY, several topologically similar classes of compounds with other heteroatoms, e.g. N–B–O compounds like ketopyrroles **2** [1,4], or N–B–C derivatives of traditional azo-dyes **3** [7] have recently been found to possess intense fluorescence as well. The idea of boron linking a potential electron

pair donating atom, while substituting H from another proton donating atom in the case of ketopyrrole derivatives **2**, has been widely exploited in a series of recent works with excellent results, see e.g. compound **4**, Scheme 2 [8]. Other heterocyclic derivatives of classic dyes with N–B–O fragments have been patented much earlier, **5–7**, Scheme 2 [9], but no photophysical properties have been reported, to the best of our knowledge.

We dedicate our attention to the design of a series of so far unknown heterocycles, boratriazines **8–11**, Scheme 3, which could ameliorate some of the above shortcomings of BODIPY dyes. No compound of this class has been reported so far, and no 1,2,3,6-boratriazine derivatives are commercially available, to the best of our knowledge. All boratriazine compounds described here are the result of our own molecular design. As long as molecular symmetry is among the reasons for the latter shortcomings, the choice of nonsymmetrical boratriazine molecules would seem appropriate. No special provisions seem necessary to obtain these compounds in order to improve their spectral sensitivity to medium effects and enhance the Stokes' shift, while their expected significant molecular polarity would be a better prerequisite to solubility in polar solvents and even water.

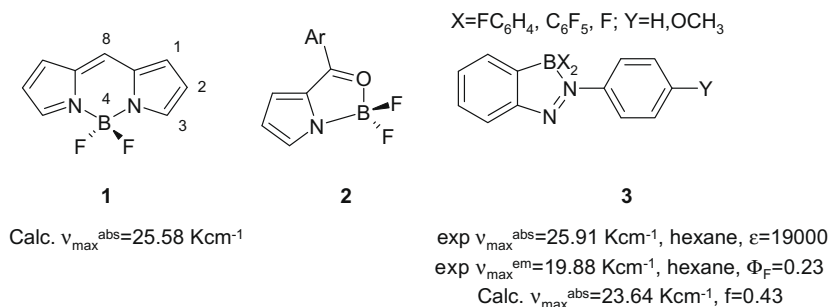
The basic tool for the intended molecular design consists of diverse quantum chemical calculations for the prediction of electronic absorption and emission spectra. Literature data indicate that UV–Vis absorption spectra of broad varieties of molecules can be routinely predicted with a precision better than 0.2 eV, or approximately 1500 cm^{−1}, taking full account for the solvent effects [10–15]. Similar calculations of molecular fluorescence spectra are presently less straightforward [14–16].

Synthesis of boratriazines **8–11** is presumably straightforward, which is the main reason for our present choice. More compounds of diverse structures will be scrutinized further.

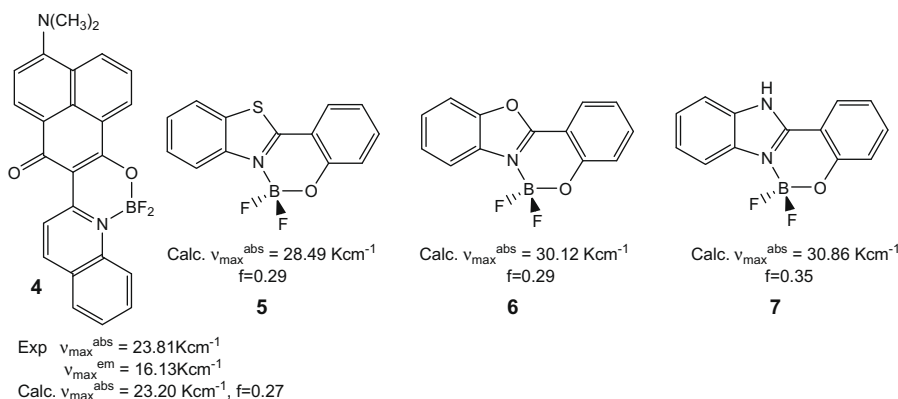
This Letter focuses on a detailed theoretical investigation of electron spectroscopic properties of compound **8**. For the validation of our computational predictions milligram amounts

* Corresponding author. Address: Institute of Organic Chemistry with Centre of Phytochemistry, Bulgarian Academy of Sciences, Acad. G. Bonchev Str., Block 9, 1113 Sofia, Bulgaria. Fax: +359 2 8700225.

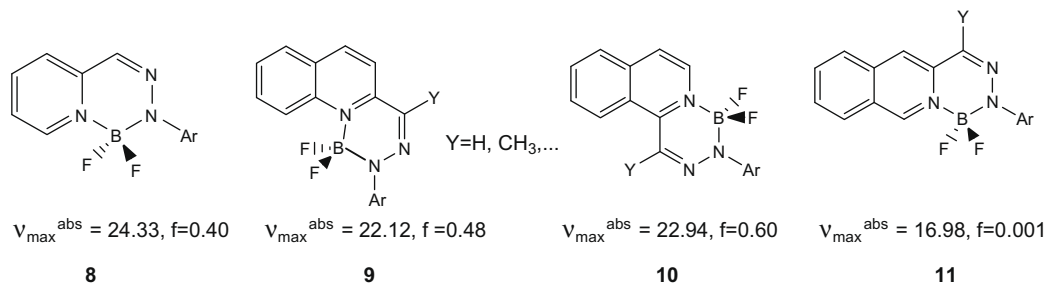
E-mail address: kaneti@orgchm.bas.bg (J. Kaneti).



Scheme 1. N–B–N linked and related chromophores. Compounds **1** and **2** are unknown [1]. Experimental data for **3** refer to the compound with $X = \text{C}_6\text{F}_5$, $Y = \text{H}$; Φ_F , fluorescence quantum yield [7]. All computations reported in this letter are single point TD PBE0/6-311+G(2d,p)//PBE0/6-311G(d,p) gas phase Franck–Condon absorption energies, unless explicitly stated otherwise. The results for **1** refer to $X = \text{F}$, $Y = \text{H}$; f , oscillator strength.



Scheme 2. N–B–O linked chromophores and corresponding TD PBE0/6-311+G(2d,p) gas phase Franck–Condon absorption energies. Experimental data for **4** are from Ref. [8]. Compounds **5–7** are mentioned in [9].



Scheme 3. Designed novel boratrimazine N–B–N molecules and their predicted gas phase energies ($\bar{\nu} \times 10^3 \text{ cm}^{-1}$) and oscillator strengths (f), TD PBE0/6-311+G(2d,p), of the longest wavelength S_0 – S_1 Franck–Condon absorptions. Results for **8** are shown for $X = Y = \text{H}$; $\text{Ar} = \text{C}_6\text{H}_5$.

of compound **8** have been synthesized upon our request and some of its photophysical characteristics have been registered experimentally.

2. Computational and experimental details

TD (Tamm-Dancoff approximation, TDA) DFT calculations of absorption spectra (singlet excitation energies) in gas phase are carried out using the GAUSSIAN 03 [17] and ORCA programs [18], using the generalized gradient hybrid PBE0 functional [19,20] and the double-hybrid correlation functional B2PLYP [21–23] at the respective completely relaxed geometries. Ground state molecular geometries are initially optimized at the 6-311G(d,p) basis set level [24,25], using PBE0 and B2PLYP. The solvent effects are modeled through the continuum dielectric PCM [26] and the COSMO conductor-like [27] approaches for the PBE0 and B2PLYP case, respectively. Single point TD B2PLYP/6-311++G(2d,2p) COSMO

calculations, as well as TD PBE0/6-311+G(2d,p) PCM calculations, are carried out at the optimized ground state geometries as mentioned above. For the emission energies, TD DFT optimizations of the first excited singlet state are carried out using GAMESS [28], with analytical TD DFT gradients for PBE0 and B3LYP functionals in the gas phase. (6,6) MCSCF calculations with six electrons in six orbitals for the ground S_0 and the first excited S_1 electronic states of **8** are also carried out with GAMESS. Finally, single point calculations of S_0 – S_1 , respectively S_1 – S_0 vertical absorption and fluorescence emission energies at the corresponding S_0 and S_1 optimized geometries are done with the symmetry adapted cluster – configuration interaction method, SAC-CI [29–31], as implemented in GAUSSIAN 03.

UV–Vis absorption spectra of compound **8**, N_2 -phenyl-1,1-difluorobora-pyrido-[2,1,a]-2,3,6-triazine are recorded on a Specord UV–Vis Carl Zeiss Jena spectrometer. Steady-state fluorescence emission spectra in different solvents are registered on a SLM

8100 Aminco spectrofluorimeter upon excitation at the maxima of the respective longest wavelength absorption bands. Fluorescence decay measurements at the maxima of emission bands are performed on a Time Correlated Single Photon Counting (TCSPC) FL900 Edinburgh Instruments Spectrometer. Spectrophotometric grade organic solvents and deionized water (Mili-Q system) are used in all measurements.

3. Results and discussion

Some of the computationally predicted geometry parameters of **8** are shown in Fig. 1. The pyrido-borotriazine system in its ground electronic state is approximately planar, with a slightly puckered borotriazine ring with BF_2 on top of the half-chair six-membered ring.

Normalized absorption and emission spectra of the designed compound **8** in different solvents are shown in Fig. 2. Time-resolved fluorescence intensity apparently shows a two-exponential decay, which cannot be clearly resolved due to the low observed signal. The fluorescence lifetime average is 9.6 ns in THF and decreases to 6.2 ns in water. A somewhat unexpected finding is that increase of solvent polarity leads to hypsochromic shift of the longest wavelength absorption maximum, Table 1. This ‘inverse’ solvatochromic effect is not an unusual phenomenon with donor–acceptor dyes. It appears to be observed more or less regularly with boron-containing acceptor chromophores [8], as well as with such classic, even though less used quinazoline chromophores [32].

The observed ‘inverse’ solvatochromic effect on the absorption spectra of **8** can be readily rationalized by inspection of its molecular orbitals, Fig. 3. TD DFT calculations show that the vertical S_0 – S_1 transition is dominated by the HOMO–LUMO excitation to ca. 65%, with another 10–15% contributed by the HOMO–LUMO+1 excitation. The squared CI coefficients of other excitations are usually lower than 10%. Excitation of a π -electron from HOMO to LUMO leads to increased localization of electron density on the acceptor part of the molecule, bearing the N–B–N fragment. Even stronger localization on the same B–N pyridine fragment of the chromophore should occur with excitations to the second lowest

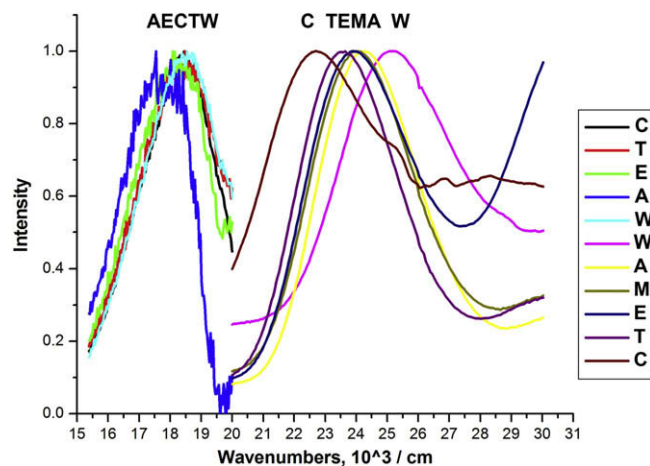


Fig. 2. Normalized absorption (right) and fluorescence (left) spectra of **8** in several solvents. Note the ‘inverse’ solvent effect on absorption, curves W and C. A much less pronounced effect is observed for the emission maxima. C, cyclohexane; T, tetrahydrofuran, E, ethanol, M, methanol, A, acetonitrile, W, water.

virtual orbital, LUMO+1, Fig. 3. This electron density localization in the lowest excited states of **8** explains the absence of bathochromic shift of the absorption maximum upon increase of solvent polarity. To further explain the origin of the observed blue shift of absorption in polar solvents, we calculate the dipole moments of the respective electronic states. The calculated dipole moment for the ground S_0 state of **8** is 6.84 D [RHF/6-31G(d,p)], while for the S_1 vertically excited state at the S_0 geometry we obtain a value of 5.57 D [CIS/6-31G(d,p)]. Corresponding DFT values are 5.43 D [S_0 , B3LYP/6-31G(d)] and 2.51 D [S_1 , TD B3LYP/6-31G(d)], respectively. Thus, the polar solvent should stabilize S_0 to a greater extent than S_1 after the vertical electronic transition and thereby increase the vertical S_0 – S_1 excitation energy by resisting the lowering of the dipole moment.

Calculated excitation energies correlate fairly well with the experimental absorption maxima energies in aprotic solvents,

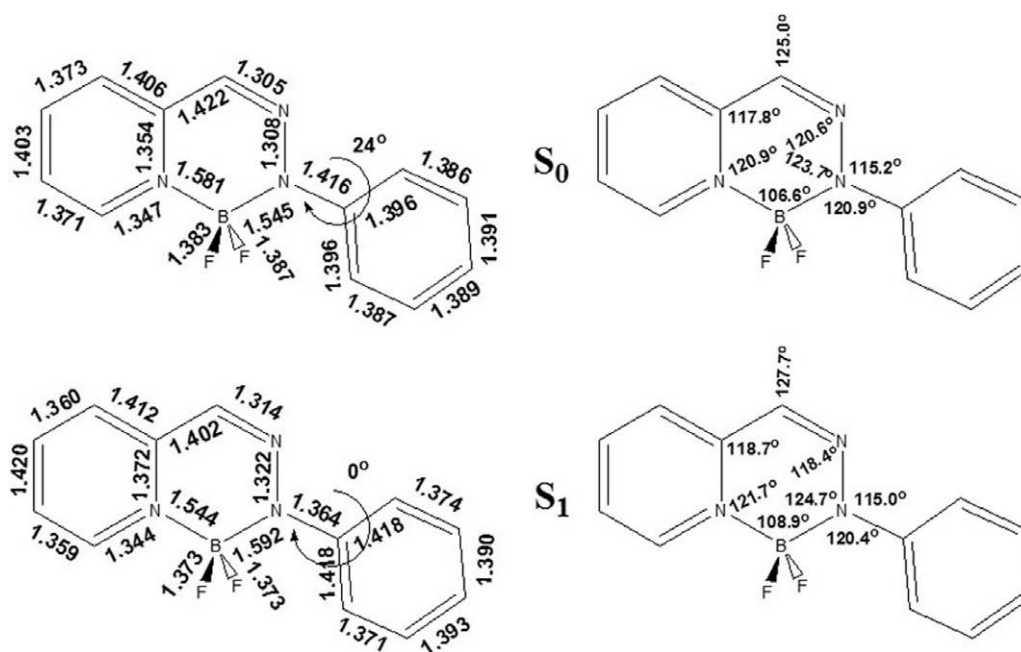


Fig. 1. Selected bond lengths and angles in **8**, PBE0/6-311G(d,p), S_0 , and CIS/6-311G(d,p), S_1 . Also shown is the dihedral twist angle between the two conjugated molecular fragments.

Table 1
Electronic spectra (wavelengths in nm; wavenumbers in cm^{-1}) and TD DFT computational predictions of transition energies to the first excited electronic state of **8** in several solvents. First singlet TD excitation energies are calculated at optimized 6-311G(d,p) geometries and PCM/PBE0, respectively COSMO/B2PLYP.

Solvent	Experiment			Computation–absorption maxima							
	Absorption λ_{max} nm	$\bar{\nu} \times 10^3 \text{ cm}^{-1}$	Emission λ_{max} nm	$\bar{\nu} \times 10^3 \text{ cm}^{-1}$	Stokes' shift, cm^{-1}	pbe0-PCM 6-311+G(2d,p) S_0 :			b2plyp – COSMO 6-311++G(2d,2p) S_0 :		
						λ_{max}	$\bar{\nu} \times 10^3 \text{ cm}^{-1}$	F_{osc}	λ_{max}	$\bar{\nu} \times 10^3 \text{ cm}^{-1}$	F_{osc}
Cyclohexane	442	22.62	543	18.42	4200	415	24.10	$f = 0.55$	419	23.87	$f = 0.59$
THF	425	23.53	541	18.48	5050	402	24.88	$f = 0.56$	401	24.94	$f = 0.60$
Ethylacetate	427	23.42				406	24.63		406	24.63	$f = 0.60$
Ethanol	418	23.92	553	18.08	5840	398	25.13	$f = 0.56$	397	25.19	$f = 0.60$
Acetone	422	23.70				398	25.13	$f = 0.56$	395	25.32	$f = 0.61$
Methanol	417	23.98				396	25.25	$f = 0.55$	396	25.25	$f = 0.61$
Acetonitrile	412	24.27	555 ^a	18.02 ^a	6250	396	25.25	$f = 0.55$	396	25.25	$f = 0.60$
Water	396	25.25	539	18.55	6700	394	25.38	$f = 0.59^b$	392	25.51	$f = 0.61$

^a Very weak and noisy emission.

^b Solvation modeling via PCM TD DFT calculation: $24.63 \times 10^3 \text{ cm}^{-1}$, $f = 0.43$ with bound H_2O at N_2 – gas phase model, TD pbe0/aug-cc-pVTZ $25.64 \times 10^3 \text{ cm}^{-1}$, $f = 0.59$, bound H_2O at N_2 , PCM(H_2O)/TD pbe0/6-311+G(2d,p) $25.52 \times 10^3 \text{ cm}^{-1}$, $f = 0.61$, bound H_2O at N_2 , COSMO(H_2O)/TD b2plyp/6-311+G(2d,2p).

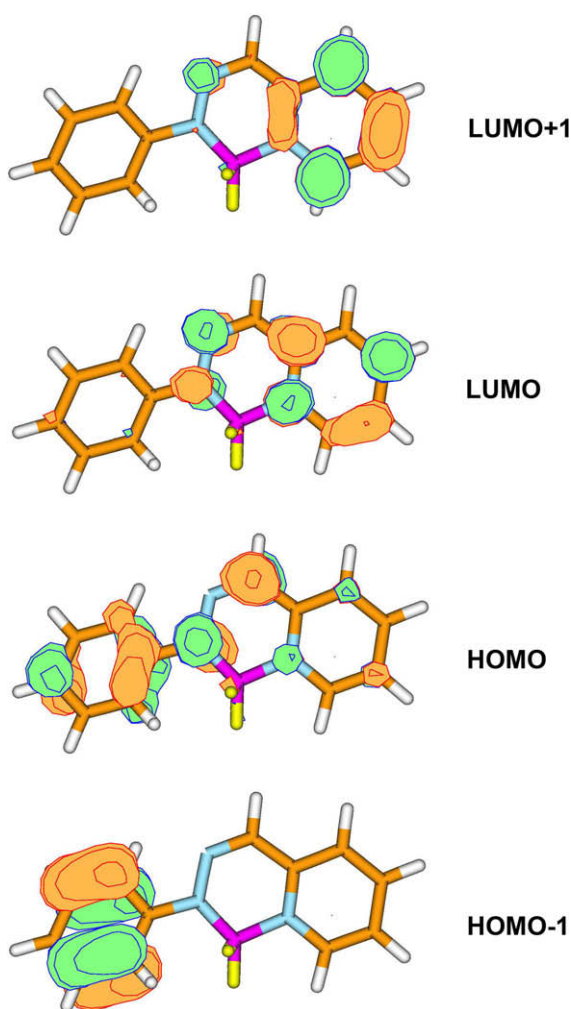


Fig. 3. PBE0/6-311G(d,p) frontier orbitals of **8** with the largest contributions to the vertical S_0 - S_1 transition.

reproducing the observed ‘inverse’ solvatochromic effect, Fig. 4. Statistically, the double-hybrid B2PLYP functional performs somewhat better than the GGA hybrid PBE0 in this particular case. The comparison of lowest singlet excitation energies computed at slightly different basis set levels, TD B2PLYP/6-311++G(2d,2p) and TD PBE0/6-311+G(2d,p), is legitimate, as far as 6-311+G(2d,p) is anyway about the convergence region of these values [10–12,14]. In fact, we also calculated PCM TD PBE0/6-

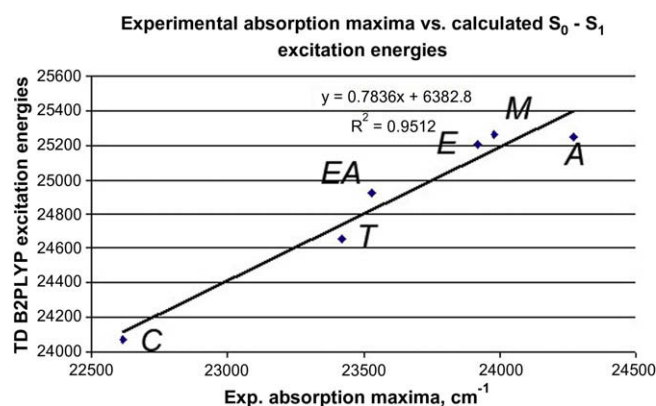


Fig. 4. Experimental and calculated COSMO TD B2PLYP/6-311++G(2d,2p)//B2PLYP/6-311G(d,p) energies of the longest wavelength absorption maximum of **8** in several solvents; EA, ethylacetate. For the remaining abbreviations, see Fig. 2.

311+G(2d,2p) singlet excitation energies for **8** in cyclohexane and acetonitrile and obtained the same values as these listed in Table 1. To the contrary, however, calculated longest wavelength absorption maxima energies for the spectra of **8** in protic solvents are almost identical, and even practically insensitive to the change of alcoholic solvent with water, Table 1. Small differences in the positions of absorption maxima in methanol and acetonitrile are an indication against protonation at the unsubstituted N_3 of the chromophores, see also Table 1. Thus, the absorption maximum in water is off the relationship for other solvents and is not included in Fig. 4 since at the moment we cannot exclude chemical changes of **8** in this solvent.

Calculated dipole moment changes for vertical fluorescence transitions at the fully relaxed S_1 geometry are respectively 7.78 D, S_1 and 2.22 D, S_0 , TD PBE0/6-311G(d,p). Single point TD B2PLYP/6-311++G(2d,2p) calculations at the above geometries give for S_1 a dipole moment of 9.02 D, while for S_0 the computed value is 6.30 D (DFT density); 5.79 (relaxed MP2 density), B2PLYP/6-311+G(2d,2p). Thus, the emission maxima should again show hypsochromic effects with increased solvent polarity, which has not been unequivocally observed in present experiments. In any case, with the experimentally observed minimal solvent effects on the fluorescence emission of **8**, we come to an increase of the observed Stokes' shift from 4200 cm^{-1} in cyclohexane to 5650 cm^{-1} in acetonitrile and 6700 cm^{-1} in the most polar solvent used, water.

The low fluorescence efficiency in solution can be explained on the basis of the computational predictions of the molecular

structure of **8**. The S_0 electronic state has a nonplanar equilibrium structure, with the phenyl substituent at N_2 rotated at 26° with respect to the boratriazine cycle, PBE0/6-311+G(2d,p). The S_1 state is essentially planar, with a phenyl rotation angle of 2° , TD PBE0/6-311G(d,p). The optimized MCSCF/6-31G(d) geometries, however, differ from the DFT results: both S_0 and S_1 equilibrium gas phase structures are predicted nearly planar, with the N_2 -phenyl plane twisted with respect to the pyrido-boratriazine plane to less than 5° . The calculated phenyl rotation barrier in the ground state of **8** is ca. 4.2 kcal/mol, PBE0/6-311+G(2d,p), which is practically free rotation and accounts for the weak fluorescence emission in solution. Better fluorescence efficiency of the present boratriazine system may be achieved via hindering the internal rotation and thereby the conformational channel for radiationless deactivation of the fluorescing state by bulky substituents on boron as in the case of **3** [7] or including the substituent to N_2 in a rigid structure [33].

Attempts at direct calculation of fluorescence emission energies require geometry optimization of the emitting electronic state, presumably S_1 , as the first step. This can be achieved either by single-reference methods as CIS [34] or TD DFT [28] or by multiconfiguration MC SCF [28] methods. At present, multi-reference CI calculations do not seem feasible for this purpose. Next, the vertical S_1 - S_0 emission energy can be conveniently calculated by TD DFT or SAC-CI methods [16]. We note that theoretical emission energies obtained by any of aforementioned methods are systematically higher than experimental values, even though theory and experiment correlate reasonably with each other. In the case of **8**, gas phase 6×6 MCSCF/6-31G(d) geometries give a SAC-CI S_0 - S_1 excitation energy of $34.57 \times 10^3 \text{ cm}^{-1}$, while the calculated SAC-CI S_1 - S_0 emission energy is $25.40 \times 10^3 \text{ cm}^{-1}$, i.e. the predicted Stokes' shift is almost 9200 cm^{-1} , more than twice larger than the observed in cyclohexane. B3LYP/6-311G geometries give an excitation energy of $31.72 \times 10^3 \text{ cm}^{-1}$ and an emission energy of $31.39 \times 10^3 \text{ cm}^{-1}$, i.e. a Stokes' shift of 430 cm^{-1} , an order of magnitude less than observed. The calculated SAC-CI emission energy at the TD PBE0/6-311G S_1 geometry is $20.47 \times 10^3 \text{ cm}^{-1}$, which best theoretical value is some 2000 cm^{-1} higher than the experiment. Presently, studies of solvent effects on molecular fluorescing states are still at the development stage before entering the arsenal of traditional methods of computational chemistry [15,35].

4. Conclusions

Preliminary quantum chemical calculations, more specifically TD (TDA) DFT, are a reliable tool in the design of unusual chromophores at the border of organic and inorganic compounds. Indeed, time-resolved photophysics of **8** and similar molecules is out of the reach of single-reference TD DFT calculations, and requires more detailed experiments, as well as multi-reference quantum chemical analysis. Nevertheless, we may confidently predict electron absorption and steady-state fluorescence properties of compounds **9–11** as given in this work. Designed properties of **8** meet the initial targets in terms of solvatochromic effects on absorption spectra, but are significantly short of the desired bright fluorescence.

Acknowledgments

This work has been inspired by Professor A. Ulises Acuña, Instituto de Química Física 'Rocasolano', C.S.I.C., 28006 Madrid. Milligram amounts of compound **8** have been synthesized upon our request by Dr. V. Kurteva, IOCCP, Sofia. The synthesis and identification of **8** will be published elsewhere. JK thanks the UAH for the Giner de los Rios Visiting Professorship. Computational work and fluorescence experiments at the UAH have been supported, respectively, via projects CTQ2006-07643 and CTQ2008-03149 of the Spanish Ministerio de Ciencia e Innovación. At the IOCCP, computations are done mainly on the facilities of the EGEE GRID computational network.

Appendix A. Supplementary material

Supplementary data associated with this article can be found, in the online version, at doi:10.1016/j.cplett.2009.07.075.

References

- [1] A. Loudet, K. Burgess, Chem. Rev. 107 (2007) 4891.
- [2] G. Ulrich, R. Ziessel, A. Harriman, Angew. Chem. Int. Ed. 47 (2008) 1184.
- [3] R. Ziessel, G. Ulrich, A. Harriman, New J. Chem. 31 (2007) 496.
- [4] M.K. Kuimova et al., Nature Chem. 1 (2009) 69.
- [5] J.-Y. Liu, H.-S. Yeung, W. Xu, X. Li, D.K.P. Ng, Org. Lett. 10 (2008) 5421.
- [6] M.J. Therien, Nature 458 (2009) 716.
- [7] J. Yoshino, N. Kano, T. Kawashima, ChemComm (2007) 559.
- [8] Y. Zhou, Y. Xiao, S. Chi, X. Qian, Org. Lett. 10 (2008) 633.
- [9] T. Padmanathan, US Patent (1974) 3793,337. Ger. Offen. (1970) 1 926 925.
- [10] D. Jacquemin, J. Preat, V. Wathelet, J.M. Andre, E.A. Perpète, Chem. Phys. Lett. 405 (2005) 429.
- [11] D. Jacquemin, E.A. Perpète, G. Scuseria, I. Ciofini, C. Adamo, J. Chem. Theory Comput. 4 (2008) 123.
- [12] D. Jacquemin, E.A. Perpète, I. Ciofini, C. Adamo, Acc. Chem. Res. 42 (2009) 326.
- [13] V. Barone, R. Improta, N. Rega, Acc. Chem. Res. 41 (2008) 605.
- [14] D. Jacquemin, E.A. Perpète, X. Assfeld, G. Scalmani, M.J. Frisch, C. Adamo, Chem. Phys. Lett. 438 (2007) 208.
- [15] B. Menucci, C. Capelli, C.A. Guido, R. Cammi, J. Tomasi, J. Phys. Chem. A 113 (2009) 3009.
- [16] T. Tsuji, M. Onoda, Y. Otani, T. Ohwada, T. Nakajima, K. Hirao, Chem. Phys. Lett. 473 (2009) 196.
- [17] M.J. Frisch et al., GAUSSIAN 03, v. C.02, D.02, E.01, Gaussian, Inc., Wallingford CT, 2004–2007.
- [18] F. Neese, ORCA v. 2.6.35, Universität Bonn, 2008.
- [19] C. Adamo, V. Barone, J. Chem. Phys. 110 (1999) 6158.
- [20] M. Ernzerhof, G.E. Scuseria, J. Chem. Phys. 110 (1999) 5029.
- [21] S. Grimme, J. Chem. Phys. 124 (2006) 034108.
- [22] T. Schwabe, S. Grimme, Phys. Chem. Chem. Phys. 8 (2006) 4398.
- [23] S. Grimme, F. Neese, J. Chem. Phys. 127 (2007) 154116.
- [24] R. Krishnan, J.S. Binkley, R. Seeger, J.A. Pople, J. Chem. Phys. 72 (1980) 650.
- [25] T. Clark, J. Chandrasekhar, P.v.R. Schleyer, J. Comp. Chem. 4 (1983) 294.
- [26] V. Barone, M. Cossi, J. Phys. Chem. A 102 (1998) 1995.
- [27] F. Eckert, A. Klamt, AlChE J. 48 (2002) 369.
- [28] M.S. Gordon, M.W. Schmidt, GAMESS v. Jan. 12, 2009, in: C.E. Dykstra, G. Frenking, K.S. Kim, G.E. Scuseria (Eds.), 'Theory and Applications of Computational Chemistry: the First Forty Years', Elsevier, Amsterdam, 2005, p. 1167.
- [29] H. Nakatsuji, Chem. Phys. Lett. 59 (1978) 362.
- [30] M. Ehara, Y. Ohtsuka, H. Nakatsuji, M. Takahashi, Y. Udagawa, J. Chem. Phys. 122 (2005) 234319 1.
- [31] H. Nakatsuji, M. Ehara, J. Chem. Phys. 122 (2005) 194108 1.
- [32] J.J. Aaron, A. Tine, M.D. Gaye, C. Parkanyi, C. Boniface, T.W.N. Bieze, Spectrochim. Acta A 47 (1991) 419.
- [33] L. Wu, K. Burgess, J. Am. Chem. Soc. 130 (2008) 4089.
- [34] J.B. Foresman, M. Head-Gordon, J.A. Pople, M.J. Frisch, J. Phys. Chem. 96 (1992) 135.
- [35] G. Scalmani, M.J. Frisch, B. Menucci, J. Tomasi, R. Cammi, V. Barone, J. Chem. Phys. 124 (2006) 094107.